# Deep Affinity Network for Multiple Object Tracking

ShiJie Sun, Naveed Akhtar, HuanSheng Song, Ajmal Mian, Mubarak Shah

Abstract—Multiple Object Tracking (MOT) plays an important role in solving many fundamental problems in video analysis in computer vision. Most MOT methods employ two steps: Object Detection and Data Association. The first step detects objects of interest in every frame of a video, and the second establishes correspondence between the detected objects in different frames to obtain their tracks. Object detection has made tremendous progress in the last few years due to deep learning. However, data association for tracking still relies on hand crafted constraints such as appearance, motion, spatial proximity, grouping etc. to compute affinities between the objects in different frames. In this paper, we harness the power of deep learning for data association in tracking by jointly modeling object appearances and their affinities between different frames in an end-to-end fashion. The proposed Deep Affinity Network (DAN) learns compact; yet comprehensive features of pre-detected objects at several levels of abstraction, and performs exhaustive pairing permutations of those features in any two frames to infer object affinities. DAN also accounts for multiple objects appearing and disappearing between video frames. We exploit the resulting efficient affinity computations to associate objects in the current frame deep into the previous frames for reliable on-line tracking. Our technique is evaluated on popular multiple object tracking challenges MOT15, MOT17 and UA-DETRAC. Comprehensive benchmarking under twelve evaluation metrics demonstrates that our approach is among the best performing techniques on the leader board for these challenges. The open source implementation of our work is available at https://github.com/shijieS/SST.git.

Index Terms—Multiple object tracking, Deep tracking, Deep affinity, Tracking challenge, On-line tracking.

# 1 Introduction

Object tracking is one of the long-standing problems in computer vision [1], [2], [3]. The techniques for this task either track a single object in videos, thereby called Single Object Trackers [4]; or multiple objects simultaneously, hence termed Multiple Object Trackers [3]. Tracking is an essential component of various vision applications, e.g. robotics, surveillance; while it also provides footholds to several high-level vision tasks, e.g. people counting [5], action recognition [6], and pose estimation [7]. Simultaneous tracking of multiple objects in videos is a comprehensive undertaking that requires detection and localization of objects in individual video frames, and associating them over an extended time to trace their trajectories.

In multiple object tracking, the natural division of subtasks between object detection and their association across different frames has led researchers to take significant advantage of existing object detectors [8], [9], [10], [11]. Modern multiple object detectors, such as Faster-RCNN [8] and YOLO [9], [10] are able to perform their task at near real-time speed while maintaining high accuracies. The continuous advances in detection frameworks have allowed the tracking literature to focus more on the problem of associating the detected objects in video frames to estimate their tracks. This work also leverages the existing detectors and concentrates on tracing the trajectories of pre-detected objects in videos.

A widely used contemporary pipeline of tracking methods [12], [13], [14], [15], [16] first computes a representation model of the detected objects or their tracklets. Later, that model is used to estimate similarities between the objects across the video frames to estimate their tracks.

The approaches following this pipeline exploit several distinct types of representation models, including; appearance models [16], [17], [18], [19], motion models [20], [21], [22], [23], and composite models [15], [24], [25]. The appearance models focus on computing easy-to-track object features that encode appearances of local regions of objects or their bounding boxes [26], [27], [28]. Currently, most of such features remain hand-crafted that also fail to consider multiple levels of abstraction of appearance. Consequently, techniques based on appearance models often struggle when similar looking objects must be tracked, especially under occlusions.

The motion models encode object dynamics to predict object locations in the future frames. Most motion modeling techniques [20], [29], [30] use linear motion models under constant velocity assumption [20]. These models usually exploit the smoothness of object's velocity, position or acceleration in the video frames. Motion model based tracking has also witnessed few attempts that account for non-linearity [31] to better represent the complexity of real-world motions. Nevertheless, both linear and non-linear models fail to handle long inter-frame object occlusions well. Moreover, they are also challenged by the scenarios of complex motions. Hence, composite model based tracking [15], [24], [25] aims at striking a balance between motion and appearance modeling. However, such a balance is hard to achieve in real-world scenarios [32].

To address the challenges of multiple object tracking, we leverage the representation power of Deep Learning [33]. We propose a Deep Affinity Network (DAN), as shown in Fig. 1, that jointly learns target object appearances and their affinities in a pair of frames in an end-to-end fashion. The appearance modeling accounts for hierarchical feature

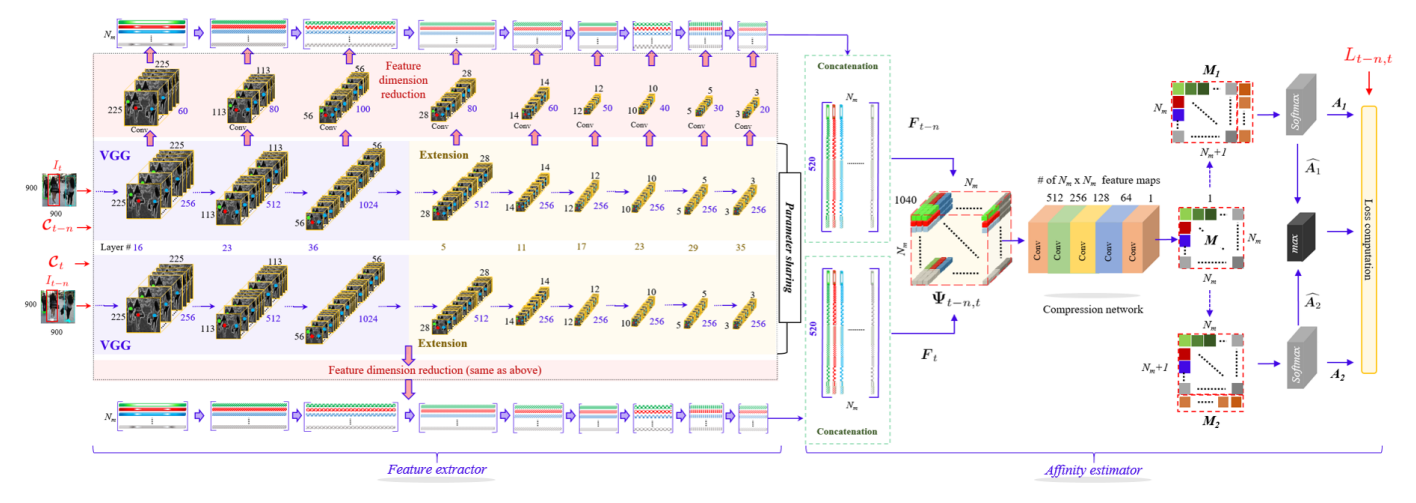


Fig. 1: Schematics of Deep Affinity Network (DAN): A pair of n time stamps apart video frames  $I_t$ ,  $I_{t-n}$  are input to the network along with the sets of centers  $\mathcal{C}_t$ ,  $\mathcal{C}_{t-n}$  of pre-detected objects in those frames. The frame pair is processed by two streams of convolution layers with shared parameters, where each stream forms an extended VGG-like network. The feature maps of nine selective layers are reduced using  $1 \times 1$  convolutional kernels. Compact features extracted from those maps are concatenated to form 520-dimensional feature vectors. Exhaustive permutations of those vectors in the feature matrices  $F_t$  and  $F_{t-n}$  are encoded in a tensor  $\Psi_{t-n,t} \in \mathbb{R}^{1040 \times N_m \times N_m}$ , where  $N_m$  is the number of objects in each frame. The tensor  $\Psi_{t-n,t}$  is mapped to a matrix  $M \in \mathbb{R}^{N_m \times N_m}$  using five convolution layers. To account for multiple identities leaving and entering between the frames,  $M_1$  and  $M_2$  are formed by appending an extra column and an extra row to M. Row- and column-wise softmax is performed over  $M_1$  and  $M_2$  respectively, and the resulting matrices  $A_1$ ,  $A_2$  are employed in network loss computation using the ground truth data association matrix  $L_{t-n,t}$ . For an input pair of frames, we compute object affinities using the predicted matrices  $A_1$  and  $A_2$ .

learning of objects and their surroundings at multiple levels of abstraction. The DAN estimates affinities between the objects in a frame pair under exhaustive permutations of their compact features. The computed affinities also account for the cases of multiple objects entering or leaving the videos between the two frames. This is done by enabling the softmax layer of DAN to separately look forward and backward in time for un-identifiable objects in the frame pair. We propose an appropriate loss function for DAN to account for this unique ability. The DAN models object appearance with a two-stream convolutional network with shared parameters and uses it to extract features to latter estimate object affinities. The overall network, does not assume the input frame pairs to appear consecutively in a video. This promotes robustness against object occlusions in the induced model.

We exploit the efficient affinity computation by the proposed deep network to associate objects in a given video frame to the objects in multiple previous frames for reliable trajectory generation using the Hungarian algorithm [34]. This results in accurate on-line multiple object tracking. The proposed approach performs tracking at 6.3 frames per second on the popular MOT15 [35], MOT17 [36] and UADETRAC [37], [38] challenge datasets, while surpassing the existing leading approaches on majority of the evaluation metrics. Our technique significantly outperforms its nearest competitors for on-line multiple pedestrian tracking.

The rest of the paper is organized as follows: In Section 2, we review the related literature and datasets of multiple object tracking. In Section 3, we introduce our tracking technique and present the DAN. Section 4 details the results of our approach on tracking challenges. We provide imple-

mentation details of our technique in Section 5, and present ablations analysis in Section 6. Conclusions are drawn in Section 7.

# 2 RELATED WORK

Tracking is a main stream problem in computer vision, hence numerous contributions in tracking can be found in the literature. In particular, Multiple Object Tracking (MOT) has attracted significant interest of researchers in recent years. For a general review of MOT, we refer to [39], where Luo et al. organized the existing literature under multiple criteria and summarized the recent techniques based on the components of tracking problem. We also refer to the survey by Emami et al. [40] who viewed multiple object tracking as an assignment problem and unified a variety of tracking approaches under this formulation. Below, we focus more on the contributions that see MOT from a data association perspective, and also review recent deep learning based techniques in MOT that relate to our method.

Many recent techniques in multiple object tracking follow a more generic 'tracking-by-detection' framework [41] that first detects target objects in video frames, and then associates them in different frames. Due to parallel developments of multiple object detectors, approaches following this line of action focus more on the data association aspect of tracking. These techniques can be broadly categorizes as local and global tracking methods. The local methods [42], [43], [44] generally consider only two frames for data association. This makes them computationally efficient, however, their performance is susceptible to tracking-irrelevant factors such as camera motion, and pose variation etc.

In contrast to local methods, global techniques [45], [46], [47] perform data association using a larger number of frames. Few global methods also cast data association into a network flow problem [48], [49], [50], [51]. For instance, Berclaz et al. [50] solved a constrained flow optimization problem for multiple object tracking, and used k-shortest paths algorithm for associating the tracks. Chari et al. [52] added a pairwise cost to the min-cost network flow framework and proposed a convex relaxation solution with a rounding heuristic for tracking. Similarly, Shitrit et al. [51] used multi-commodity network flow for MOT. Although popular, this line of methods rely on object detectors rather strongly [41] that makes it less desirable for scenarios where occlusions are encountered frequently. In their work, Shu et al. [44] handled occlusions up to a scale by extending a part based human detector [53]. There have also been attempts to use dense detections without non-maximum suppression for tracking [54], [55]. One major goal of such techniques is to mitigate the problems caused by occlusions and close proximity of the targets that are not handled well by the detectors.

Another technique to mitigate the shortcomings of object detectors is to make use of on-line trainable classifier for the target objects [56], [57], [58]. Application of on-line classifiers has seen some success in the context of single object tracking. However, it has failed to gain popularity in MOT, and has only been successfully applied in limited scenarios [59]. There are also other instances of MOT under tracking-by-detection framework that explicitly focus on mitigating the adverse affects of occlusions. Milan et al. [60] employed a continuous energy minimization framework for MOT that incorporates occlusion explicit reasoning and appearance modeling. To handle occlusions and clutter, Wen et al. [25] proposed a data association technique based on undirected hierarchical relation hyper-graph. Bochinski et al. [61] leveraged the intersection-over-union and predefined thresholds for the association of objects in frames. Focusing on computational efficiency, they showed acceptable tracking performance with a speed of up to 100 fps. Chen et al. [62] proposed a multiple hypothesis tracking method by accounting for scene detections and detection-detection correlations between video the frames. Their method is claimed to handle false trajectories while dealing with close object hypotheses.

Deep learning based tracking methods [63], [64], [65], [66], [67] often represent objects using the models that are pre-trained for other tasks in computer vision, and associate objects using them for tracking. For instance, Bertinetto et al. [63] proposed to use a fully convolutional Siamese Network [68] in the context of single object tracking. Similarly, Bea et al. [24] modified the Siamese Network to learn discriminative deep representations for multiple object tracking with object association. They combined on-line transfer learning with the modified network to fine-tune the latter for on-line tracking. Son et al. [64] proposed a quadruplet convolutional neural network that learns to associate objects detected in different video frames. Their network is used by a minimax label propagation method to associate the targets. Schulter et al. [65] also proposed a network that is trained for data association in the context of multiple object tracking. Feichtenhofer et al. [66] proposed a multi-function

CNN for simultaneous detection and tracking under the detection framework R-FCN [69]. Insafutdinov et al. [67] proposed deep learning based method for pose estimation and tracking. They trained a model that groups body parts and tracks a person using the head joint. However, their method under performs if heads are occluded.

In the context of deep learning, one important aspect of MOT research is the collection and annotation of data itself. Dedicated works have appeared in this area. A summary of the existing multiple object tracking datasets can be found in [39]. Two datasets are particularly relevant to our work, namely MOT dataset [70] and UA-DETRAC dataset [37]. The MOT dataset introduced by Milan et al. [70] is used by a popular recent multiple object tracking challenge MOT17 (https://motchallenge.net/ data/MOT17/). The dataset provides a variety of real-world videos for pedestrian tracking. The UA-DETRAC challenge (https://detrac-db.rit.albany.edu/) uses the large scale UA-DETRAC dataset that contains videos of vehicle traffic in real-world conditions. We provide further details on both datasets in Section 4. Other popular datasets for object tracking include KITTI [71] and PETS [72].

Until recently, most of the deep learning based methods have dealt with single object tracking instead of MOT. Moreover, in tracking-by-detection framework for MOT, deep learning is mainly exploited in appearance modeling. The data association component of the problem is yet to benefit from deep learning, especially in a manner that the learned association model is also tailored to appearance modeling. This work fills this gap by jointly modeling the appearance of objects in a pair of frames and learning their associations in those frames in an end-to-end manner. The proposed Deep Affinity Network performs comprehensive appearance modeling and uses it further to estimate object affinities in the frame pair. The efficient affinity computation allows our technique to look back deep into the previous frames for object association. This keeps the proposed technique robust to object occlusions for tracking.

#### 3 Proposed Approach

Multiple Object Tracking is a challenging problem that involves detection of objects, extracting their features, computing affinities between them and simultaneously tracing multiple object trajectories in videos. We capitalize on the representation power of deep learning to perform these tasks for on-line tracking. Central to our tracker is a CNN-based Deep Affinity Network (DAN), see Fig. 1, that jointly models object appearances and their affinities across two different frames that are not necessarily adjacent. The overall approach exploits the efficient affinity estimation by DAN to associate objects in the current frame to those in multiple previous frames to compute reliable trajectories. We provide a detailed discussion on our approach below. However, we first introduce some notations and conventions for a concise description in the text and figures.

# **Notations:**

- I<sub>t</sub> denotes the t<sup>th</sup> video frame under 0-based indexing.
- t-n:t denotes an interval from t-n to t.

- A subscript t n, t indicates that the entity is computed for the frame pair  $I_{t-n}$ ,  $I_t$ .
- $C_t$  is the set of center locations of the objects in the  $t^{\text{th}}$  frame with  $C_t^i$  as its  $i^{\text{th}}$  element.
- F<sub>t</sub> is the feature matrix associated with the t<sup>th</sup> frame, where its i<sup>th</sup> column F<sub>t</sub><sup>i</sup> is the feature vector of the i<sup>th</sup> object in that video frame.
- $\Psi_{t-n,t}$  is a tensor encoding all possible pairings of the columns of  $F_{t-n}$  and  $F_t$  along its depth dimension.
- $L_{t-n,t}$  denotes a binary data association matrix encoding the correspondence between the objects detected in frames  $I_{t-n}$  and  $I_t$ . If object '1' in  $I_{t-n}$  corresponds to the  $n^{\text{th}}$  object in  $I_t$ , then the  $n^{\text{th}}$  element of the first row of  $L_{t-n,t}$  is non-zero.
- $A_{t-n,t}$  is an affinity matrix encoding similarities between the bounding boxes in  $(t-n)^{\text{th}}$  frame and the  $t^{\text{th}}$  frame.
- $\mathcal{T}_t$  denotes the set of trajectories or tracks until the  $t^{\text{th}}$  time stamp. The  $i^{\text{th}}$  element of this set is itself a set of 2-tuples, containing indices of frames and detected objects. For example,  $\mathcal{T}_t^i = \{(0,1),(1,2)\}$  indicates the short track connecting the  $1^{\text{st}}$  object in  $0^{\text{th}}$  frame and the  $2^{\text{nd}}$  object in  $1^{\text{st}}$  frame.
- Z(·) is an operator that computes the number of elements in a set/matrix in its argument.
- $\Lambda_t \in \mathbb{R}^{\mathcal{Z}(\mathcal{T}_{t-1}) \times (\mathcal{Z}(\mathcal{C}_t)+1)}$  is an accumulator matrix whose coefficient at index (i,j) integrates the affinities of the  $i^{\text{th}}$  identity in track set  $\mathcal{T}_{t-1}$  to the  $j^{\text{th}}$  object in the  $t^{\text{th}}$  frame over previous  $\delta_b$  frames.
- N<sub>m</sub> denotes the allowed maximum number of objects in a frame, and B denotes the batch size during training.

# **Conventions:**

The shape of the output at each network layer is described as  $Batch \times Channel \times Width \times Height$ . For the sake of brevity, we often leave out the Batch dimension.

#### 3.1 Object detection and localization

The proposed framework leverages the advances in multiple object detection [8], [73] to identify and locate the objects of interest in video frames. The detection stage in our approach expects video frames as inputs and provides a set of bounding boxes for the target objects in those frames. We compute the object center locations  $C_t$  using the available bounding boxes. The performance of our approach is evaluated for on-line challenges in multiple object tracking (see Section 4) that provide their own detectors for the objects of interest. For the MOT17 challenge [36], we use the provided Faster R-CNN [8] and SDP [74] detectors; for MOT15 [35] we use [75]; and for the UA-DETRAC [37], [38], we use the EB detector [73]. Our choices are entirely based on the on-line challenges for multiple object tracking that enable fair benchmarking of our approach. However, the proposed framework is compatible with other existing multiple object detectors as well. Since our main contribution is in object tracking and not detection; we refer to the original works for details on the used detectors.

# 3.2 Deep Affinity Network (DAN)

We model the appearance of objects in video frames and compute their cross-frame affinities using the Deep Affinity Network (DAN), shown in Fig. 1. To align our discussion with the existing tracking literature, we present the proposed network as two components; (a) Feature extractor, and (b) Affinity estimator, however, the overall network is end-to-end trainable. The DAN training requires video frame  $I_t$  along with its object centers  $C_t$ ; and video frame  $I_{t-n}$  along with its object centers  $\mathcal{C}_{t-n}$  as inputs. Notice that, we do not restrict the two frames to appear consecutively in video. Instead, we allow them to be n time stamps apart, such that  $n \in \mathbb{N} \stackrel{\text{rand}}{\sim} [1, N_V]$ . Whereas our network is eventually deployed to track objects in consecutive video frames, training it with non-consecutive frames benefits the overall approach in reliably associating objects in a given frame to those in multiple previous frames. DAN also requires ground truth binary data association matrix  $L_{t-n,t}$  of the input frame pair for computing the network cost during training. The inputs to DAN are shown in red color in Fig. 1. We describe working details of the internal components of our network below after discussing the data preparation.

## 3.2.1 Data preparation

Multiple object tracking datasets e.g. [36], [38] often lack in fully capturing the aspects of camera photometric distortions, background scene variations and other practical factors to which tracking approaches should remain robust. For model based approaches, it is important that the training data contains sufficient variations of such tracking-irrelevant factors to induce robustness in the learned models. Hence, we perform the following preprocessing steps over the available data.

- 1) Photometric distortions: Each pixel of a video frame is first scaled by a random value in the range [0.7, 1.5]. The resulting image is converted to HSV format, and its Saturation channel is again scaled by a random sample in [0.7, 1.5]. The frame is then converted back to RGB format and rescaled by a random sample in the same range. This process of photometric distortion is similar to [76], that also inspires the used range values.
- 2) Frame expansion: We expand the frames by a random ratio sampled in the range [1,1.2]. The expansion results in increasing frame sizes. We fill the pixels added to the expanded frames with the mean pixel value of the data.
- 3) *Cropping*: We crop the frames using cropping ratios randomly sampled in the range [0.8, 1]. We keep only those crops that contain the center points of all the detected boxes in the original frames.

Each of the above steps is applied to the frame pairs sequentially with a probability 0.3. The frames are then resized to fixed dimensions  $H \times W \times 3$ , and horizontally fliped with a probability of 0.5. The overall strategy of modifying the training data is inspired by Liu et al. [76] who alter images to train an object detector. However, different from [76], we simultaneously process two frames by applying the abovementioned transformations to them.

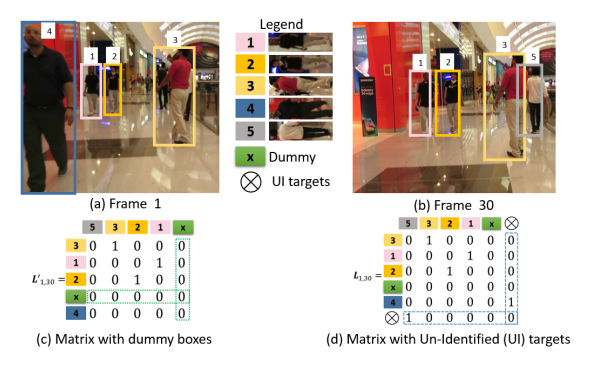


Fig. 2: Illustration of data association matrix between frame 1 and 30, with  $N_m=5$ . Frame 1 and 30 in (a) and (b) jointly contain 5 detected objects. (c) Creation of an intermediate matrix that considers dummy objects (rows and columns with zeros) to achieve  $N_m=5$  per frame. (d) Augmentation with extra column and row to include Un-Identified (UI) targets (objects leaving and entering respectively) between the two frames.

TABLE 1: The input data for training DAN. The tensor dimensions are expressed as Channels  $\times$  Height  $\times$  Width.

Input	Dimensions/Size
$I_{t-n}$ , $I_t$	$3 \times H \times W$
$L_{t-n,t}$	$1 \times (N_m + 1) \times (N_m + 1)$
$\mathcal{C}_t$ , $\mathcal{C}_{t-n}$	$N_m$

The resulting processed frames are used as inputs to the DAN along with the associated object centers computed by a detector. We compute the data association matrices for the frames by introducing an upper bound  $N_m$  on the maximum number of objects allowed in a given frame. In our experiments,  $N_m = 80$  proved a generous bound for the benchmark challenges. For consistency, we introduce additional rows and columns (with all zeros) in the data association matrix corresponding to dummy bounding boxes in each video frame so that all the frames eventually contain  $N_m$  objects and the matrix size is  $N_m \times N_m$ . Figure 2 illustrates the construction of data association matrix used in our approach, where we let  $N_m = 5$  for simplicity. Frames 1 and 30 contain four detected persons each amounting to five distinct identities. Fig. 2c shows the construction of an intermediate matrix  $m{L}'_{1,30}$  for the frames with a dummy row and column for dummy bounding boxes. In Fig. 2d, the association matrix is augmented with an extra row and a column, labeled as un-identified targets (UI targets). The augmented column accounts for currently tracked objects leaving the video and the augmented row accounts for new objects entering the video. We eventually use the form of ground truth association matrix shown in Fig. 2d to train the DAN. In the shown illustration, the last column of the augmented matrix has a 1 for object-4 because it has left and the last row has a 1 for object-5 because it has appeared in Frame 30. Notice that, using this convention, DAN is able to account for multiple objects leaving and entering the video i.e. by placing 1's at multiple rows in the last column and by placing 1's at multiple columns in the last row, respectively. After data preparation, the entities available as inputs to our network are summarized in Table 1.

TABLE 2: Architectural details of the *Extension & Compression* networks in Fig. 1: I.C denotes the number of input channels for a layer, O.C is the number of output channels, S is the stride size, B.N (Y/N) indicates if the Batch Normalization is applied; and ReLU (Y/N) indicates if the ReLU activation is used. Strides and Paddings are the same in both spatial dimensions.

Sub-network	Index	I.C	O.C	Kernel	S	Padding	B.N	ReLU
	0	1024	256	$1 \times 1$	1	0	Y	Y
	3	256	512	$3 \times 3$	2	1	Y	Y
	6	512	128	$1 \times 1$	1	0	Y	Y
	9	128	256	$3 \times 3$	2	1	Y	Y
Extension	12	256	128	$1 \times 1$	1	0	Y	Y
(Feature extractor)	15	128	256	$3 \times 3$	2	1	Y	Y
· ·	18	256	128	$1 \times 1$	1	0	Y	Y
	21	128	256	$3 \times 3$	2	1	Y	Y
	24	256	128	$1 \times 1$	1	0	Y	Y
	27	128	256	$3 \times 3$	2	1	Y	Y
	30	256	128	$1 \times 1$	1	0	Y	Y
	33	128	256	$3 \times 3$	2	1	Y	Y
	0	1040	512	$1 \times 1$	1	0	Y	Y
	3	512	256	$1 \times 1$	1	0	Y	Y
Compression	6	256	128	$1 \times 1$	1	0	Y	Y
(Affinity estimator)	9	128	64	$1 \times 1$	1	0	N	Y
,	11	64	1	$1 \times 1$	1	0	N	Y

#### 3.2.2 Feature extractor

We refer to the first major component of the DAN as feature extractor for its functionality. This sub-network models comprehensive yet compact features of the detected objects in video frames. As shown in Fig. 1, the feature extraction is performed by passing pairs of video frames and object centers through two streams of convolution layers. These streams share the model parameters in our implementation, whereas their architecture is inspired by VGG16 network [77]. We use the VGG architecture after converting its fully-connected and softmax layers to convolution layers. This modification is made because the spatial features of objects, which are of more interest in our task, are better encoded by convolution layers. Compared to the original VGG16, the input frame size for our network is much larger (i.e.  $3 \times 900 \times 900$ ) due to the nature of the task at hands and the available tacking datasets. Consequently, we are still able to compute  $56 \times 56$  feature maps after the last layer of the modified VGG network. In Fig. 1, we index the last layer of VGG as the 36th layer under the convention that Batch Normalization [78] and ReLU activations [79] are counted as separate layers. We refer to [77] for the details on the original VGG architecture.

We reduce the spatial dimensions of our feature maps beyond  $56 \times 56$ , after the VGG layers, by introducing further convolution layers. The 36-layer *Extension* network (see Fig. 1) gradually reduces feature maps to size  $3 \times 3$ . The architectural details of the extension network are provided in the top half of Table 2. The table counts the output of VGG network as the input to the first layer of the extension that is indexed 0. Since the Batch Normalization and ReLU are counted as separate layers, the first column of the table increments indexes with step size 3.

Knowing the object center locations in the input frames (as  $C_t$  and  $C_{t-n}$ ) allows us to extract center pixels of the objects as their representative features. We extend this notion to the feature maps of our network and sample the

TABLE 3: Details of feature dimension reduction layers in Fig. 1: 3 layers are selected from VGG network. 6 layers are selected from the Extension network. I.C denotes the number of input channels. S.D indicates spatial dimensions of feature maps. O.C is the number of output channels.

Sub-network	Layer index	I.C	S.D	O.C
	16	256	255x255	60
VGG	23	512	113x113	80
	36	1024	56x56	100
	5	512	28x28	80
	11	256	14x14	60
Extension network	17	256	12x12	50
Extension network	23	256	10x10	40
	29	256	5x5	30
	35	256	3x3	20

maps of different convolution layers at object centers after accounting for the reduction in spatial dimensions of the maps. Due to multiple sequential convolution operations along the network layers, the sampled vectors represent object features at different levels of abstraction. This occurs due to the fact that the receptive field of sequentially applied convolution kernels increases as we go deeper in the network. This effect is exacerbated by pooling which reduces the spatial dimensions of feature maps ensuring that the features sampled from latter layers additionally account for full objects and even their surroundings. These are highly desirable characteristics of features for tracking. To ensure such features are sufficiently expressive, it remains imperative to learn a large number of feature maps. However, this would make the comprehensive feature vector formed by combining features from multiple layers too large to be practically useful.

We side-step this issue by reducing the number of feature maps of nine empirically selected layers in our network. This reduction is performed with additional convolution layers branching out from the two main streams of the feature extractor (see Fig. 1). The additional layers use  $1 \times 1$ convolution kernels for dimensionality reduction. Table 3 lists indices of the selected nine layers along the number of channels at the input and output of the convolution layers performing the dimensionality reduction. Our network concatenates feature vectors from the selected nine layers to form a 520-dimensional vector for a detected object. By allowing  $N_m$  detections in the  $t^{\text{th}}$  frame, we obtain a feature matrix  $\mathbf{F}_t \in \mathbb{R}^{520 \times N_m}$ . Correspondingly, we also construct  $\boldsymbol{F}_{t-n} \in \mathbb{R}^{520 \times N_m}$  for the  $(t-n)^{\text{th}}$  frame. Recall that these matrices also contain features for dummy objects that actually do not exist in the video frames. We implement these features as zero vectors.

## 3.2.3 Affinity estimator

The objective of this component of DAN is to encode affinities between the objects using their extracted features. To that end, the network arranges the columns of  $F_t$  and  $F_{t-n}$  in a tensor  $\Psi \in \mathbb{R}^{N_m \times N_m \times (520 \times 2)}$ , such that the columns of the two feature matrices are concatenated along the depth dimension of the tensor in  $N_m \times N_m$  possible permutations, see Fig. 1 for illustration. We map this tensor to a matrix  $M \in \mathbb{R}^{N_m \times N_m}$  through a compression network that uses 5 convolution layers with  $1 \times 1$  kernels. Specifications of this network are given in the bottom half of Table 2.

The architecture of the compression network is inspired by the physical significance of its input and output signals. The network maps a tensor encoding combinations of object features to a matrix that codes similarities between the features (hence, the objects). Thus, it performs a gradual dimension reduction along the depth of the input tensor with convolutional kernels that do not allow neighboring elements of feature maps to influence each other. For a moment, consdier a forward-pass through the DAN until the computation of  $M \in \mathbb{R}^{\hat{N}_m \times N_m}$ . We can see that the predicted M must subsequently be compared to the ground truth data association matrix  $L_{t-n,t}$  for loss computation. However, unlike  $L_{t-n,t}$ , M does not account for the objects entering or leaving the video between the input frames. To take care of those cases, we also append an extra column and an extra row to M to form matrices  $M_1 \in \mathbb{R}^{N_m \times (N_m+1)}$  and  $M_2 \in \mathbb{R}^{(N_m+1) \times N_m}$ , respectively. This is analogous to the augmentation of  $L_{t-n,t}$  explained in Section 3.2.1. However, here we separately append the row and column vectors to M in order to keep the loss computation welldefined and physically interpretable. The vectors appended to M take the form  $\mathbf{v} \in \mathbb{R}^{N_m} = \gamma \mathbf{1}$ , where  $\mathbf{1}$  is a vector of ones, and  $\gamma$  is a hyper-parameter of the proposed DAN.

#### **Network loss:**

For DAN, the  $m^{\text{th}}$  row of the augmented matrix  $M_1$ associates the  $m^{\text{th}}$  identity in frame  $I_{t-n}$  to  $N_m+1$  identities in frame  $I_t$ , where +1 results from the UI-targets. We fit a separate probability distribution over each row of  $M_1$ by applying a *row*-wise softmax operation over the matrix. Thus, rows of the resulting matrix  $oldsymbol{A}_1 \in \mathbb{R}^{N_m imes (N_m+1)}$ encode probabilistic associations between each object in frame  $I_{t-n}$  and all identities in frame  $I_t$ , including the unidentified objects in the latter frame. We correspondingly apply a *column*-wise softmax operation over  $M_2$  to compute  $A_2 \in \mathbb{R}^{(N_m+1) imes N_m}$  whose columns signify similar backwards associations from frame  $I_t$  to  $I_{t-n}$ . We emphasize that the proposed encoding of probabilistic associations between the two frames allows for multiple objects entereing or leaving the video between the frames. The maximum number of entering/leaving objects is upper-bounded by  $N_m$  - the maximum number of allowed objects in a frame.

We define the loss function for DAN with the help of four sub-losses, referred to as 1) Forward loss  $\mathcal{L}_f$ : that encourages correct identity association from frame  $I_{t-n}$ to frame  $I_t$ . 2) Backward Loss  $\mathcal{L}_b$ : that ensures correct associations from  $I_t$  to  $I_{t-n}$ . 3) Consistency loss  $\mathcal{L}_c$ : to rebuff any inconsistency between  $\mathcal{L}_f$  and  $\mathcal{L}_b$ . 4) Assemble loss  $\mathcal{L}_a$ : that supresses non-maximum forward/backward associations for affinity predictions. Concrete definitions of these losses are provided below:

$$\mathcal{L}_{f}(\boldsymbol{L}_{1}, \boldsymbol{A}_{1}) = \frac{\sum_{\substack{\text{mat\_el} \\ \text{mat el}}} (\boldsymbol{L}_{1} \odot (-\log \boldsymbol{A}_{1}))}{\sum_{\substack{\text{mat el} \\ \text{el}}} (\boldsymbol{L}_{1})}$$
(1)

$$\mathcal{L}_{f}(\boldsymbol{L}_{1}, \boldsymbol{A}_{1}) = \frac{\sum_{\text{mat\_el}} (\boldsymbol{L}_{1} \odot (-\log \boldsymbol{A}_{1}))}{\sum_{\text{mat\_el}} (\boldsymbol{L}_{1})}$$

$$\mathcal{L}_{b}(\boldsymbol{L}_{2}, \boldsymbol{A}_{2}) = \frac{\sum_{\text{mat\_el}} (\boldsymbol{L}_{2} \odot (-\log \boldsymbol{A}_{2}))}{\sum_{\text{mat\_el}} (\boldsymbol{L}_{2})}$$

$$(2)$$

$$\mathcal{L}_c(\widehat{A}_1, \widehat{A}_2) = ||\widehat{A}_1 - \widehat{A}_2||_1 \tag{3}$$

$$\mathcal{L}_a(oldsymbol{L}_3, \widehat{oldsymbol{A}}_1, \widehat{oldsymbol{A}}_2) = rac{\sum\limits_{ ext{mat\_el}} \left(oldsymbol{L}_3 \odot \left(-\log(\max(\widehat{oldsymbol{A}}_1, \widehat{oldsymbol{A}}_2))
ight)
ight)}{\sum\limits_{ ext{mat\_el}} (oldsymbol{L}_3)}$$

$$\mathcal{L} = \frac{\mathcal{L}_f + \mathcal{L}_b + \mathcal{L}_a + \mathcal{L}_c}{4}.$$
 (5)

In the above equations,  $L_1$  and  $L_2$  are the trimmed versions of  $L_{t-n,t}$  constructed by ignoring the last row and column of that matrix, respectively.  $\widehat{A}_1$  and  $\widehat{A}_2$  denote the matrices  $A_1$  and  $A_2$  trimmed to the size  $N_m \times N_m$  by dropping the last column and last row respectively. Similarly,  $L_3$  drops out both last row and column of  $L_{t-n,t}$ . The operator  $\odot$  denotes Hadamard product, and  $\sum\limits_{\text{mat\_el}}$  (.) sums coefficients of the matrix in its argument. The max and log operations are also performed element-wise.

We compute the final loss  $\mathcal{L}$  as the mean value of the four sub-losses. The overall cost function of our network is defined as the Expected value of the training data loss. The afore-mentioned four sub-losses are carefully designed for our problem. In the Forward and Backward losses, instead of forcing  $A_q$ , where  $q \in \{1,2\}$ ; to approximate corresponding  $L_q$  by using a distance metric, we maximize the probabilities encoded by the relevant coefficients of  $A_q$ . We argue that this strategy is more sensible than minimizing a distance between a binary matrix  $(L_q)$  and a probability matrix  $(A_q)$ . Similarly, given the difference between  $A_1$  and  $A_2$  is expected to be small, we employ  $\ell_1$ -distance instead of more commonly used  $\ell_2$ -distance for the Consistency loss. Once the DAN is trained, we use it to compute the affinity matrix for an input frame pair as  $A \in \mathbb{R}^{N_m \times N_m + 1} = \mathcal{A}(\max(\widehat{A_1}, \widehat{A_2}))$ , where  $\mathcal{A}(.)$ appends the  $(N_m+1)^{\text{th}}$  column of  $A_1$  to the matrix in its argument. The max operation used in our definition of the affinity matrix A also justifies the maximization performed to compute the Assemble loss. Thus, the four sub-losses defined above are complementary that result in a systematic approximation of the ground truth data association.

#### 3.3 DAN deployment

Whereas the *feature extractor* component of DAN is trained as a two-stream network, it is deployed as a one-stream model in our approach. This is possible because the parameters are shared between the two streams. In Fig. 3, we illustrate the deployment of DAN by showing its two major components separately. The network expects a single frame  $I_t$  as its input, along the object center locations  $C_t$ . The feature extractor computes the feature matrix  $F_t$  for the frame and passes it to the affinity estimator. The latter uses the feature matrix of a previous frame, say  $I_{t-n}$  to compute the permutation tensor  $\Psi_{t-n,t}$  for the frame pair. The tensor is then mapped to an affinity matrix by a simple forward pass through the network and a concatenation operation, as described above. Thus each frame is passed through the object detector and feature extractor only once, but the features are used multiple times for computing affinities with multiple other frames in pairs.

# 3.4 Deep track association

To associate objects in the current frame with multiple previous frames, we store feature matrices of the frames with their time stamps. After frame 0, that initializes our approach and results in  $F_0$ , we can compute affinities between the objects in the current frame and those in any previous frame using their feature matrices. As illustrated in Fig. 3, the computed affinity matrices are used to update trajectory sets by looking back deep into the previous frames.

Deep track association is performed as follows. We initialize our track set  $\mathcal{T}_0$  with as many trajectories as the number of detected objects in  $I_0$ . A trajectory here is a set of 2-tuples, each containing the time stamp of the frame and the object identity. The trajectory set is updated at the  $t^{\text{th}}$  time stamp with the help of Hungarian algorithm [34] applied to an accumulator matrix  $\Lambda_t \in \mathbb{R}^{\mathcal{Z}(\mathcal{T}_{t-1}) \times (\mathcal{Z}(\mathcal{C}_t) + 1)}$ . The used accumulator matrix integrates the affinities between objects in the current frame and the previous frames. A coefficient of  $\Lambda_t$  at index (i,j) is the sum of affinities of the  $i^{\text{th}}$  identity in the track set  $\mathcal{T}_{t-1}$  to the  $j^{\text{th}}$  object in the  $t^{\text{th}}$  frame for the previous  $\delta_b$  frames, where  $\delta_b$  is a parameter of our approach.

At each time stamp, we are able to efficiently compute up to  $\delta_b$  affinity matrices using the DAN to look back into the existing tracks. We let  $\delta_b=t$  in Fig. 3 for simplification. One subtle issue in successfully applying the Hungarian algorithm to our problem is that we allow multiple objects to leave a video between its frames. Therefore, multiple trajectories could be assigned to the *single* UI-target column allowed in our accumulator matrix (inherited from the affinity matrices). We handle this issue by repeating the last column of  $\Lambda_t$  until every trajectory in  $\mathcal{T}_{t-1}$  gets assigned to a unique column of the augmented matrix<sup>1</sup>. This ensures that all un-identified trajectories can be mapped to un-identified objects.

Overall, our tracker is an on-line approach in the sense that it does not use future frames to predict object trajectories. Hence, it can be used with continuous video streams. One practical issue in such cases is that very long tacks may result over large time intervals. The parameter  $\delta_b$  also bounds the maximum number of time stamps we associate with a track. We remove the oldest node in a track if the number of frames for its trajectory exceed  $\delta_b$ . Similarly, for the objects disappearing from a video, we allow a waiting time of  $\delta_w$  frames before removing its trajectory from the current track set. We introduce these parameters in our framework for purely pragmatic reasons. Their values can be adjusted according to the on-board computational and memory capacity of a tracker.

# 4 EXPERIMENTS

In this section, we evaluate the proposed approach on three well-known multiple object tracking challenges, namely Multiple Object Tracking 17 (MOT17) [70], Multiple Object Tracking 15 (MOT15) [35] and UA-DETRAC [37], [38]. All of these are on-line challenges where tracking results are computed by a hosting server, once a new technique is

1. The number of columns of augmented  $\Lambda_t$  are allowed to exceed  $N_m+1$ . However, it does not have any ramifications as that matrix is only utilized by the Hungarian algorithm.

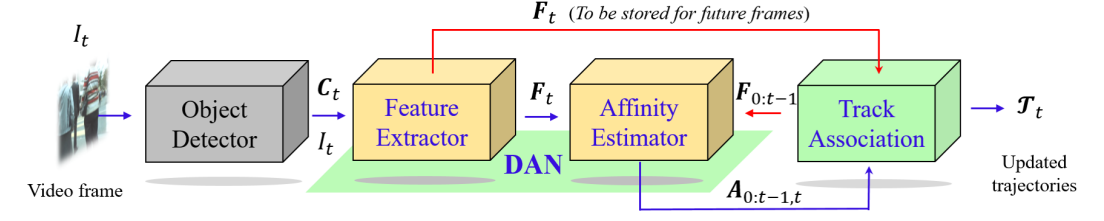


Fig. 3: Deep tracking with DAN deployment: For the  $t^{\text{th}}$  frame  $I_t$ , the object centers  $C_t$  provided by the detectors are used to compute the feature matrix  $F_t$  with *one* stream Feature Extractor of DAN. The  $F_t$  is paired with each of the last t feature matrices  $F_{0:t-1}$ , and each pair is processed by the Affinity Estimator to compute the same number of affinity matrices  $A_{0:t-1,t}$ . The  $F_t$  is also stored for computing affinity matrices in the future. The trajectory set  $\mathcal{T}_t$ , is updated by associating the current frame with t previous frames using the computed affinity matrices.

TABLE 4: Attributes of MOT17 training data [36]. The last three columns indicate the number of detected boxes by the detectors in complete video. 'Density' denotes the average number of pedestrian per frame, and 'Move' indicates if the video is recorded by a moving camera (Y) or not (N).

Video Index	Resolution	FPS	Length (frames)	Boxes	Tracks	Density	Move	<b>DPM</b> [53]	SDP [74]	FRCNN [8]
02	$1920 \times 1080$	30	600	18581	62	31.0	N	7267	11639	8186
04	$1920 \times 1080$	30	1050	47557	83	45.3	N	39437	37150	28406
05	$640 \times 480$	14	837	6917	133	8.3	Y	4333	4767	3848
09	$1920 \times 1080$	30	525	5325	26	10.1	N	5976	3607	3049
10	$1920 \times 1080$	30	654	12839	57	19.6	Y	8832	9701	10371
11	$1920 \times 1080$	30	900	9436	75	15.5	Y	8590	7509	6007
13	$1920 \times 1080$	25	750	11642	110	8.3	Y	5355	7744	8442

submitted for evaluation. Annotated training data is provided for learning the models, however, labels of the test data remain inaccessible to public. The servers perform comprehensive evaluation of the submitted techniques using several standard metrics. We introduce the challenges, training datasets, and the evaluation metrics below. The performance of our approach and its comparison to other techniques currently on the leader board is also presented.

## 4.1 Multiple Object Tracking 17 (MOT17)

The Multiple Object Tracking 17 (MOT17) [70] is among the latest on-line challenges in tracking. Similar to its previous version MOT16 [36], this challenge contains seven different indoor and outdoor scenes of public places, with pedestrians as the objects of interest. A video for each scene is divided into two clips, one for training and the other for testing. The dataset provides detections of objects in the video frames with three detectors, namely SDP [74], Faster-RCNN [8] and DPM [53]. The challenge accepts both online and off-line tracking approaches, where the latter are allowed to use the future video frames to predict tracks.

#### 4.1.1 Dataset

The challenge provides seven videos for training along with their ground truth tracks and detected boxes from three detectors. The scenes vary significantly in terms of background, illumination conditions and camera view points. We summarize the main attributes of the provided training data in Table 4. As can be noticed, the provided resolution for scene 05 is different from the others. Similarly, there are also variations in camera frame rates, the average number of objects per frame (i.e. density) and the total number of tracks. Scene 07 is also captured with a lower angle that resulted in significant occlusions. All these variations make the dataset challenging.

The testing data consists of clips from the same seven scenes, excluding the training video clips. There are 17,757 frames in testing data, and it is public knowledge that there are 2,355 tracks in those clips with 564,228 boxes. However, the track labels and boxes are not available publicly, and evaluation is performed by the host server in private.

## 4.1.2 Evaluation metrics

We benchmark our approach comprehensively using twelve standard evaluation metrics, that include both CLEAR MOT metrics [80], and the MT/ML metrics [81]. We summarize these metrics in Table 5. Concrete definitions of MOTA and MOTAL are provided below:

$$MOTA = 1 - \frac{\sum_{t} (FP_t + FN_t + ID\_Sw_t)}{\sum_{t} GT_t}.$$
 (6)

$$MOTAL = 1 - \frac{\sum_{t} (FP_t + FN_t + \log_{10}(ID\_Sw_t + 1))}{\sum_{t} GT_t}.$$
 (7)

In the above equations, the subscript 't' indicates that the values are computed at the  $t^{\rm th}$  time stamp, whereas 'GT' stands for ground truth. We refer to Table 5 for the other symbols used in the equations.

#### 4.1.3 Results

We trained our DAN with the training data provided by the hosting server. Upon submission, our approach was benchmarked by the server itself. In Table 6, we summarize current results of the published techniques on the leader board taken directly from the challenge server. Whereas our method is *on-line*, the table also includes the results of best performing *off-line* methods to highlight the competitive performance of our approach. As can be seen, the

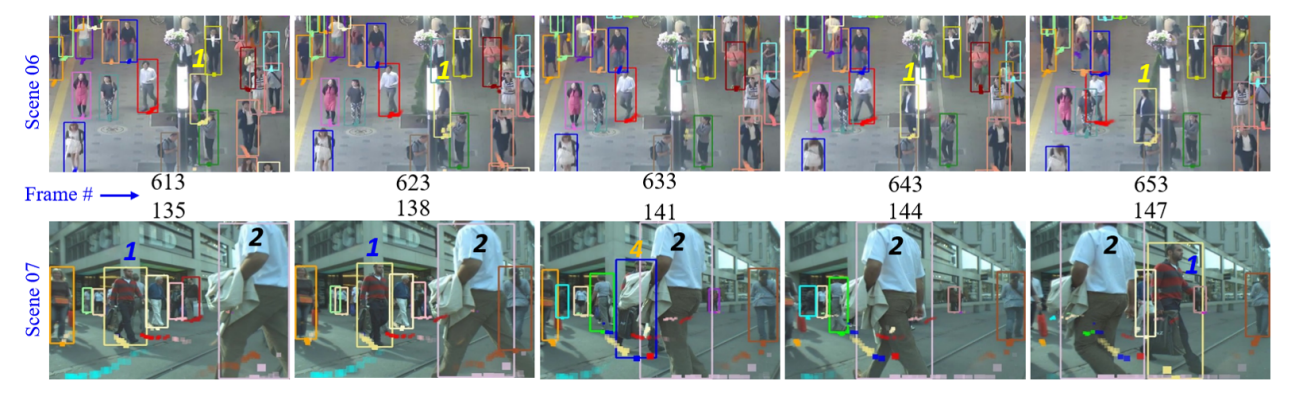


Fig. 4: Tracking example of the proposed method from MOT17 (taken from the host server). The predicted tracks are identified by the color of bounding boxes. The mentioned identity numbers are for reference in the text only. In both scenes, our approach successfully tracks identity-1 despite inter-frame occlusions. Frame 141 of Scene 07 causes a temporary mis-identification, however, our approach is able to recover well due to deep track association.

TABLE 5: Metrics used for benchmarking.

Metric	Better	Perfect	Description
MOTA	higher	100%	Overall Tracking Accuracy. See Eq. (6).
MOTAL	higher	100%	Log Tracking Accuracy. See Eq. (7).
MOTP	higher	100%	Percentage alignment of predicted bounding
			box and ground truth.
Rcll			The percentage of detected targets.
IDF1	higher	100%	F1 score of the predicted identities.
MT	higher	100%	Mostly tracked targets. The percentage of
	_		ground-truth trajectories covered by a track
			hypothesis for 80% of their life or more.
ML	lower	0	Mostly lost targets. The percentage of ground-
			truth trajectories covered by a track hypothesis
			for 20% of their life or less.
FP	lower	0	Number of false positives.
FN	lower	0	Number of false negatives.
ID_Sw.	lower	0	Identity switches, see [82] for details.
Frag	lower	0	The count of trajectory fragmentations.
Hz	higher	Inf.	Processing speed in frames per second.

proposed approach (named DAN after the network) is able to outperform the existing on-line and off-line methods on five metrics, whereas the performance generally remains competitive on the other metrics. In particular, our results are significantly better than the existing on-line methods for MOTA and MOTAL that are widely accepted as comprehensive multiple object tracking metrics.

In Fig. 4, we show two examples of our method's tracking performance on MOT17 challenge. The color of bounding boxes in the shown frames indicate the trajectory identity predicted by our tracker. The numbers mentioned on the frames are for reference in the text only. The figure presents typical examples of inter-frame occlusions occurring in tracking datasets. In scene 06 (first row), identity-1 disappears in frame 633 (and adjacent frames - not shown), and then reappears in frame 643. Our tracker is able to easily recover from this occlusion (the same color of bounding boxes). Similarly, the occlusion of identity-1 in frame 144 of scene 07 is also handled well by our approach. Our tracker temporarily misjudges the trajectory in frame 141 by assigning it a wrong identity, i.e. 4 due to severe partial occlusion. However, it is able to quickly recover from this situation by keep looking deeper into the previous frames.

# 4.2 Multiple Object Tracking 15 (MOT15)

In order to more comprehensively benchmark our technique for pedestrian tracking, we also evaluate it on Multiple Object Tracking 15 (MOT15) challenge [35] which also deals with multiple pedestrian tracking similar to MOT17. However, due to its earlier release in 2014, MOT15 benchmarks more methods as compared to MOT17. MOT15 provides 11 video sequences along with their ground truth tracks and detections using the detector proposed by Dollar et al. [75]. The provided ground truth detections do not consider object occlusions and a bounding box for a completely occluded object of interest is provided for training anyway. Such training data can be misleading for our appearance modeling based tracker. Hence, we do not train or fine-tune the DAN with MOT15 training data. Instead, we directly apply our MOT17 model to the MOT15 challenge. The hosting server computes results based on its used detector [75].

## 4.2.1 Results

There are 4 video sequences (Venice-1, ADL-Rundle-1, ADL-Rundle-3 and ETH-Crossing) in MOT15 that contain the same scenes as the video sequences 01, 06, 07 and 08 in the MOT17. For a fair comparison of our technique with the benchmarked approaches, we report the average results on these scenes in Table 7. Note that, all approaches in the table contain the corresponding training video clips of the same four scenes in their training data. The results are computed by the private hosting server of the challenge. As can be seen, the proposed approach significantly outperforms the existing methods evaluated on the MOT15 challenge on three metrics, especially on the MOTA metric.

## 4.3 UA-DETRAC

The UA-DETRAC challenge [37], [38] is based on a large-scale tracking dataset for vehicles. It comprises 100 videos that record around 10 hours of vehicle traffic. The recording is made in 24 different locations, and it includes a wide variety of common vehicle types and traffic conditions. The scenes include urban highways, traffic crossings, and T-junctions etc. Overall, the dataset contains about 140k video frames, 8,250 vehicles, and 1,210k bounding boxes. Similar

TABLE 6: MOT17 challenge results from the server: The symbol  $\uparrow$  indicates that higher values are better, and  $\downarrow$  implies lower values are favored. The proposed method is *online*. Offline methods are included for reference only.

Tracker	Type	MOTA↑	MOTAL↑	MOTP↑	Rcll↑	IDF1↑	MT↓	ML↓	FP↓	FN↓	ID_Sw↓	Frag↓	Hz↑
FWT_17 [15]	offline	51.3173	51.786	77.0024	56.0583	47.5597	21.4	35.3	24101	247921	2648	4279	0.2
jCC [83]	offline	51.1614	51.4802	75.9164	56.0777	54.4957	20.9	37.0	25937	247822	1802	2984	1.8
MHT_DAM [16]	offline	50.7132	51.1228	77.5219	55.1777	47.1803	20.8	36.9	22875	252889	2314	2865	0.9
EDMT17 [62]	offline	50.0464	50.4471	77.2553	56.1689	51.2532	21.6	36.3	32279	247297	2264	3260	0.6
MHT_bLSTM [84]	offline	47.5226	47.8887	77.4943	52.494	51.9188	18.2	41.7	25981	268042	2069	3124	1.9
IOU17 [61]	offline	45.4765	46.5371	76.8505	50.0814	39.4037	15.7	40.5	19993	281643	5988	7404	1522.9
PHD_GSDL17 [22]	online	48.0439	48.7518	77.1522	52.8641	49.6294	17.1	35.6	23199	265954	3998	8886	6.7
EAMTT [85]	online	42.6344	43.4291	76.0305	48.8728	41.7654	12.7	42.7	30711	288474	4488	5720	1.4
GMPHD_KCF [23]	online	39.5737	40.603	74.5414	49.6253	36.6362	8.8	43.3	50903	284228	5811	7414	3.3
GM_PHD [86]	online	36.3560	37.1719	76.1957	41.3771	33.9243	4.1	57.3	23723	330767	4607	11317	38.4
DAN (Proposed)	online	52.4224	53.916	76.9071	58.4225	49.4934	21.4	30.7	25423	234592	8431	14797	6.3

TABLE 7: MOT15 challenge results: The symbols ↑ and ↓ respectively indicate that higher and lower values are preferred.

Tracker	Type	MOTA ↑	MOTP ↑	IDF1 ↑	MT ↓	ML ↓	FP ↓	FN ↓	ID Sw↓	Frag ↓	HZ↑
QuadMOT [64]	offline	29.30	75.73	40.88	10.48	34.28	1022.25	3461.00	1670.97	2732.67	6.2
CNNTCM [87]	offline	23.03	73.90	34.90	7.93	41.88	1167.25	3607.50	2792.58	2606.37	1.7
SiameseCNN [88]	offline	28.78	72.90	39.70	10.83	42.20	633.00	3681.50	846.93	2020.80	52.8
MHT_DAM [16]	offline	27.58	73.53	44.50	21.30	34.60	1290.25	3223.75	1453.52	2170.06	0.7
LP_SSVM [89]	offline	21.18	73.35	36.15	8.70	37.80	1517.00	3396.00	2002.88	2342.29	41.3
AMIR15 [90]	online	31.88	73.40	44.13	11.73	22.53	1105.75	3055.75	3273.27	6360.93	1.9
HybridDAT [68]	online	31.48	75.03	46.90	19.70	27.38	1299.00	2869.00	1373.40	3674.18	4.6
AM [91]	online	30.23	72.20	46.98	12.90	46.75	510.50	3711.00	755.37	4133.45	0.5
CDA_DDALpb [24]	online	31.68	72.15	38.55	13.38	42.75	402.75	3751.75	1407.74	3088.61	2.3
SCEA [92]	online	23.85	73.08	32.65	8.03	45.78	751.50	3847.00	2220.33	3157.50	6.8
RNN_LSTM [93]	online	13.83	72.28	20.78	6.40	37.58	1779.75	3615.50	5287.59	7520.59	165.2
DAN (Proposed)	online	38.30	71.10	45.60	17.60	41.20	1290.25	2700.00	1648.08	1515.60	6.3

TABLE 8: Attributes of UA-DETRAC dataset [37], [38]. The 'Boxes' column indicates the total number of bounding boxes in videos. 'Length' is given in number of frames.

Type	Videos	Length	Boxes	Vehicles	Tracks	Density
Training	60	84k	578k	5936	5.9k	6.88
Testing	40	56k	632k	2314	2.3k	11.29

to the MOT challenges, the UA-DETRAC challenge accepts submissions of tracking approaches and the hosting server evaluates their performance on a separate test data.

#### 4.3.1 Dataset

We summarize the major attributes of the dataset in Table 8. The table contains information on both training and testing sets. The available videos have a consistent frame size of  $540 \times 960$ , and a frame rate of 25 fps. All the videos are recorded with static cameras, generally installed at high locations. Although in terms of variations this dataset may appear less challenging than MOT datasets, the larger size of data and the scenes of crossings and junctions make tracking in this dataset a difficult task.

## 4.3.2 Evaluation metrics

The evaluation metrics used by UA-DETRAC are similar to those introduced in Table 5, however, they are computed slightly differently. These metrics are abbreviated as PR-MOTA, PR-MOTP, PR-MT, PR-ML, PR-FP, PR-FN and PR-ID\_Sw, where the prefix PR indicates that the computation is done using a Precision-Recall curve. For instance, to compute PR-MOTA, the thresholds of the detectors are gradually varied to compute a 2D precision-recall curve. Then, for each point on the plot, MOTA value is estimated to get a 3D curve. The PR-MOTA is computed as the integral

score of the resulting curve. The same procedure is also adopted for computing the other PR-based metrics.

#### 4.3.3 Results

We summarize the quantitative results of our approach in the last row of Table 9. The table also reports performances of the top approaches on the leader board for UA-DETRAC challenge at the time of submission of this work. The names of methods (first column) include the detectors used by the techniques, e.g. we used the EB detector [73], hence EB+DAN. The choice of EB detector in our technique is empirical. The results in the table ascertain the overall effectiveness of the proposed approach in tracking vehicles on roads.

We also illustrate tracking results of our approach in Fig. 5 with the help of two examples. Again, the predicted trajectories are specified by the colors of bounding boxes, and the mentioned identity numbers are only for referencing in the text. In the top row (scene MVI\_40762) the EB detector fails to detect identity-2 in frame 130 - 134 (only frame 132 is shown) due to occlusion by identity-1. However, once the detection is made again, our tracker is able to assign the object correctly to its trajectory from frame 136 onwards. Similarly, in scene MVI\_40855, the detector is unable to detect identity-1 in frames 132-143 due to occlusion by identity-2. Nevertheless, when the identity-1 is detected again in frame 154, our approach assigns it to its correct trajectory. These examples demonstrate robustness of our approach to missed detection by the detector under tracking-by-detection framework.

## 5 IMPLEMENTATION DETAILS

We implement the Deep Affinity Network (DAN) using the Pytorch framework [99]. Training was performed on

TABLE 9: UA-DETRAC challenge results: The symbol ↑ indicates that higher values are better, and ↓ implies lower values are favored. The names of approaches also include the used detectors.

Name	PR-MOTA ↑	PR-MOTP↑	PR-MT ↑	PR-ML ↓	PR-FP↓	PR-FN↓	PR-ID_Sw↓	Hz↑
EB [73]+IOUT [61]	19.4	28.9	17.7	18.4	14796.5	171806.8	2311.3	6902.1
R-CNN [94]+IOUT [61]	16.0	38.3	13.8	20.7	22535.1	193041.9	5029.4	-
CompACT [95]+GOG [48]	14.2	37.0	13.9	19.9	32092.9	180183.8	3334.6	389.5
CompACT [95]+CMOT [19]	12.6	36.1	16.1	18.6	57885.9	167110.8	285.3	3.8
CompACT [95]+H2T [25]	12.4	35.7	14.8	19.4	51765.7	173899.8	852.2	3.0
RCNN [94]+DCT [96]	11.7	38.0	10.1	22.8	336561.2	210855.6	758.7	0.7
CompACT [95]+IHTLS [97]	11.1	36.8	13.8	19.9	53922.3	180422.3	953.6	19.8
CompACT [95]+CEM [98]	5.1	35.2	3.0	35.3	12341.2	260390.4	267.9	4.6
Proposed (EB [73]+DAN)	20.2	26.3	14.5	18.10	9747.8	135978.1	518.2	6.3



Fig. 5: Tracking examples from the UA-DETRAC challenge. Predicted tracks are identified by the bounding box colors and the identity numbers are for reference only. The proposed tracker is able to assign identities to their correct track (in both cases) despite missed detection in several frames due to limited performance of the detector for occluded objects.

NVIDIA GeForce GTX Titan GPU. Hyper-parameters of DAN were optimized with the help of MOT17 dataset, for which we specified a validation set to train our model. MOT17 was selected for parameter optimization due to its manageable size. The hyper-parameter values finally used in our implementation are as follows. Batch size B = 8, number of training epochs per model = 120, number of maximum objects allowed per frame  $N_m = 80$ , and  $\gamma = 10$ . We let  $N_V = 30$ . Our network uses input frame size of  $900 \times 900$ . All the training and testing data is first resized to these dimensions before passing it through the network. We used the SGD optimizer [100] for training the DAN, for which we used 0.9 and 5e-4 for the momentum and weight decay parameters respectively. We started the learning process with 0.01 as the learning rate, which we decreased to  $1/10^{th}$  of the previous value at epochs 50, 80 and 100. Once the network is trained, we still need to decide on the values of the parameters  $\delta_b$  and  $\delta_w$ . We selected the best values of these parameters with a grid search for optimal MOTA metric on our validation set. We used multiples of three in the range [3,30] to form the grid, based on which  $\delta_w=12$ and  $\delta_b = 15$  were selected in the final implementation.

#### 6 Discussion

Central to the success of our approach is the ability of DAN to reliably associate objects between pair of frames in a video. In Fig. 6, we illustrate the object association capabilities of the proposed DAN under different practical conditions. Each column of the figure shows a pair of frames

that are n time stamps apart, where n is randomly sampled from [1, 30]. The figure shows association between the objects as computed by DAN. Firstly, it can be noticed that the association is robust to large illumination variations. Secondly, DAN is able to comfortably handle significant object occlusions. Additionally, despite the existence of multiple similar looking objects, the network is able to correctly associate the objects. For instance, see Fig. 6(e) where there are multiple white and red cars but this does not cause problems.

The chosen examples in Fig. 6 are completely random. We observed the same level of performance by DAN for all the cases we tested. We argue that this robustness results from feature modeling at multiple levels of abstraction and accounting for objects' surroundings at higher abstraction levels. Such an abstraction occurs due to the increasing receptive field of convolution kernels as we go deeper in our network. Moreover, joint modeling of features and affinities across the frames also play a critical role in achieving this performance.

For an effective architecture of our network, we tested numerous intuitive alternatives. We present a few interesting choices out of those as an ablation analysis here. We choose these cases for their ability to add to our understanding the role of important components in the final network. We introduce DAN-Remove model, that removes the 'Feature dimension reduction' layers in Fig. 1 and directly concatenates the features to estimate object affinities. As another case, we replace the 'Compression network' in affinity estimator component by a single convolutional

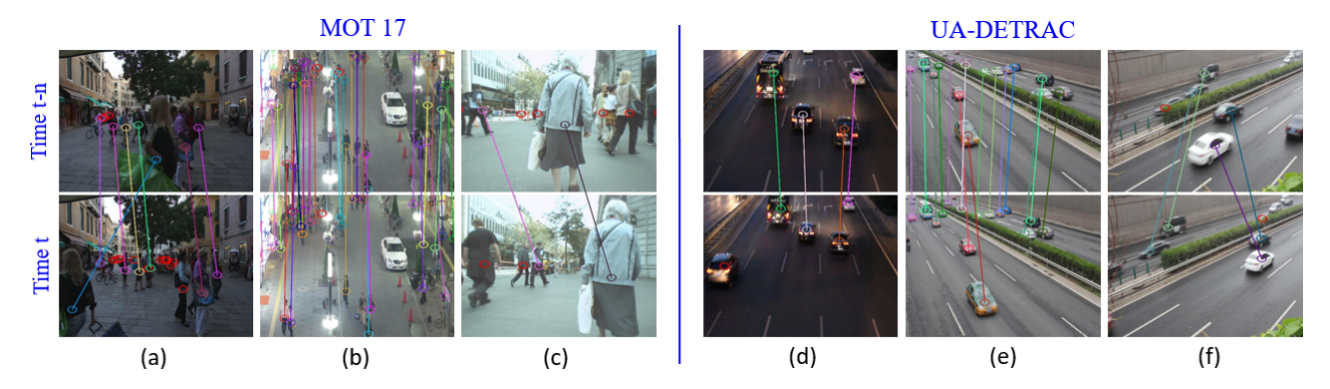


Fig. 6: Illustration of cross-frame associations based on DAN outputs. The frame pairs are randomly chosen  $n \sim [1,30]$  time-stamps apart. The association remains robust to illumination conditions, partial occlusions and existence of multiple similar looking objects in the video frames.

TABLE 10: Training losses of DAN variants at different epochs. Losses computed for MOT17 dataset.

Variant	50	80	100	110	120
DAN-Replace	0.155	0.115	0.108	0.112	0.111
DAN-Remove	0.209	0.181	0.169	0.131	0.124
DAN-Mean	0.134	0.083	0.080	0.076	0.075
DAN	0.107	0.057	0.045	0.045	0.043

layer. Hence, the resulting DAN-Replace model maps object features to affinities abruptly instead of doing it gradually. In another choice, instead of defining our ensemble loss with the *max* operation, we use the *mean* operation, and refer to the resulting network as DAN-Mean.

We provide the training loss values at different epochs for these different choices for the network in Table 10 for MOT17. It is apparent that the proposed DAN is able to converge to a better loss with less number of epochs as compared to all the other choices. The closest performance is achieved by DAN-Mean that has the same architecture as DAN but a slightly different loss function. The importance of feature compression is clear from the poor loss of DAN-Remove. Similarly, from the results of DAN-Replace, it is also apparent that gradual compression of feature maps for affinity estimation is more desirable than an abrupt compression.

# 7 CONCLUSION

We presented a multiple object tracker that performs on-line tracking by associating the objects detected in the current frame with those in multiple previous frames. The tracker derives its strength from our proposed Convolutional Neural Network architecture, referred to as Deep Affinity Network (DAN). The proposed DAN models features of predetected objects in the video frames at multiple levels of abstraction, and infers object affinities across different frames by analyzing exhaustive permutations of the extracted features. The cross-frame objects similarities and object features are recorded by our approach to trace the trajectories of the object. We evaluated our approach on three on-line multiple object tracking challenges MOT17, MOT15 and UA-DETRAC, using twelve different evaluation metrics. The proposed tracker is able to achieve excellent overall performance with the highest Multiple Object Tracking Accuracy

on all the challenges. It also achieved an average speed of 6.3 frames per second, while leading the result board as the best performing on-line tracking approach on many of the evaluation metrics.

## 8 ACKNOWLEDGEMENT

This research was supported by ARC grant DP160101458, the National Natural Science Foundation of China (Grant No. 61572083), the Joint Found of of Ministry of Education of China (Grant No. 6141A02022610), Key projects of key R & D projects in Shaanxi (Grant No. 2018ZDXM-GY-047), Team cultivation project of Central University (Grant No. 300102248402) and China Scholarship Council (CSC). The GPU used for this research was donated by NVIDIA Corporation.

# REFERENCES

- A. Yilmaz, O. Javed, and M. Shah, "Object tracking: A Survey," ACM Computing Surveys, vol. 38, no. 4, pp. 13–es, 2006.
- [2] B. Ma, L. Huang, J. Shen, and L. Shao, "Discriminative tracking using tensor pooling," *IEEE Transactions on Cybernetics*, vol. 46, no. 10, pp. 2411–2422, 2015.
- [3] J. Shen, Z. Liang, J. Liu, H. Sun, L. Shao, and D. Tao, "Multiobject Tracking by Submodular Optimization," *IEEE Transactions on Cybernetics*, 2018.
- [4] M. Mueller, N. Smith, and B. Ghanem, "Context-Aware Correlation Filter Tracking," Cvpr2017, pp. 1396–1404, 2017.
- [5] S. Sun, N. Akhtar, H. Song, C. Zhang, J. Li, and A. Mian, "Benchmark data and method for real-time people counting in cluttered scenes using depth sensors," arXiv:1804.04339, 2018.
- [6] H. Rahmani, A. Mian, and M. Shah, "Learning a Deep Model for Human Action Recognition from Novel Viewpoints," IEEE Transactions On Pattern Analysis And Machine Intelligence, Vol. 40, No. 3, March 2018 Learning, vol. 94, no. 6, pp. 667–681, 2018.
- [7] D. Zhang and M. Shah, "Human Pose Estimation in Videos," 2015 IEEE International Conference on Computer Vision (ICCV), pp. 2012–2020, 2015.
- [8] S. Ren, K. He, R. Girshick, and J. Sun, "Faster R-CNN: Towards Real-Time Object Detection with Region Proposal Networks," *IEEE Transactions on Pattern Analysis and Machine Intelligence*, vol. 39, no. 6, pp. 1137–1149, 2017.
- [9] D. Impiombato, S. Giarrusso, T. Mineo, O. Catalano, C. Gargano, G. La Rosa, F. Russo, G. Sottile, S. Billotta, G. Bonanno, S. Garozzo, A. Grillo, D. Marano, and G. Romeo, "You Only Look Once: Unified, Real-Time Object Detection Joseph," Nuclear Instruments and Methods in Physics Research, Section A: Accelerators, Spectrometers, Detectors and Associated Equipment, vol. 794, pp. 185–192, 2015.

- [10] J. Redmon and A. Farhadi, "YOLO9000: Better, Faster, Stronger," 2016.
- [11] P. Felzenszwalb, D. McAllester, and D. Ramanan, "A discriminatively trained, multiscale, deformable part model," in 26th IEEE Conference on Computer Vision and Pattern Recognition, CVPR, 2008.
- [12] W. Hu, X. Li, W. Luo, X. Zhang, S. Maybank, and Z. Zhang, "Single and multiple object tracking using log-euclidean riemannian subspace and block-division appearance model," *IEEE Transactions on Pattern Analysis and Machine Intelligence*, vol. 34, no. 12, pp. 2420–2440, 2012.
- [13] L. Zhang and L. Van Der Maaten, "Preserving structure in modelfree tracking," *IEEE Transactions on Pattern Analysis and Machine Intelligence*, vol. 36, no. 4, pp. 756–769, 2014.
- [14] Y. Xiang, A. Alahi, and S. Savarese, "Learning to track: Online multi-object tracking by decision making," in *Proceedings of the IEEE International Conference on Computer Vision*, vol. 2015 Inter, 2015, pp. 4705–4713.
- [15] R. Henschel, L. Leal-Taixé, D. Cremers, and B. Rosenhahn, "Fusion of Head and Full-Body Detectors for Multi-Object Tracking," Computer Vision and Pattern Recognition Workshops (CVPRW), 2018.
- [16] C. Kim, F. Li, A. Ciptadi, and J. M. Rehg, "Multiple hypothesis tracking revisited," in *Proceedings of the IEEE International Confer*ence on Computer Vision, vol. 2015 Inter, 2015, pp. 4696–4704.
- [17] S. Zhang, X. Lan, H. Yao, H. Zhou, D. Tao, and X. Li, "A Biologically Inspired Appearance Model for Robust Visual Tracking," IEEE Transactions on Neural Networks and Learning Systems, 2016.
- [18] H. Nam and B. Han, "Learning Multi-Domain Convolutional Neural Networks for Visual Tracking," Cvpr, pp. 4293–4302, 2015.
- [19] S. H. Bae and K. J. Yoon, "Robust online multi-object tracking based on tracklet confidence and online discriminative appearance learning," Proceedings of the IEEE Computer Society Conference on Computer Vision and Pattern Recognition, pp. 1218–1225, 2014.
- [20] M. D. Breitenstein, F. Reichlin, B. Leibe, E. Koller-Meier, and L. Van Gool, "Robust tracking-by-detection using a detector confidence particle filter," *Proceedings of the IEEE International Conference on Computer Vision*, no. Iccv, pp. 1515–1522, 2009.
- [21] F. Fleuret, J. Berclaz, R. Lengagne, and P. Fua, "Multicamera people tracking with a probabilistic occupancy map," *IEEE Transactions on Pattern Analysis and Machine Intelligence*, vol. 30, no. 2, pp. 267–282, 2008.
- [22] Z. Fu, P. Feng, S. M. Naqvi, and J. A. Chambers, "Particle PHD filter based multi-target tracking using discriminative group-structured dictionary learning," in ICASSP, IEEE International Conference on Acoustics, Speech and Signal Processing Proceedings, 2017, pp. 4376–4380.
- [23] T. Kutschbach, E. Bochinski, V. Eiselein, and T. Sikora, "Sequential sensor fusion combining probability hypothesis density and kernelized correlation filters for multi-object tracking in video data," in 2017 14th IEEE International Conference on Advanced Video and Signal Based Surveillance, AVSS 2017, 2017.
- [24] S. H. Bae and K. J. Yoon, "Confidence-Based Data Association and Discriminative Deep Appearance Learning for Robust Online Multi-Object Tracking," *IEEE Transactions on Pattern Analysis and Machine Intelligence*, vol. 40, no. 3, pp. 595–610, 2018.
- [25] L. Wen, W. Li, J. Yan, Z. Lei, D. Yi, and S. Z. Li, "Multiple target tracking based on undirected hierarchical relation hypergraph," Proceedings of the IEEE Computer Society Conference on Computer Vision and Pattern Recognition, vol. 1, pp. 1282–1289, 2014.
- Vision and Pattern Recognition, vol. 1, pp. 1282–1289, 2014.
  [26] C. H. Kuo, C. Huang, and R. Nevatia, "Multi-target tracking by on-line learned discriminative appearance models," in Proceedings of the IEEE Computer Society Conference on Computer Vision and Pattern Recognition, 2010, pp. 685–692.
- [27] H. Izadinia, I. Saleemi, W. Li, and M. Shah, "(MP)2T: Multiple people multiple parts tracker," in Lecture Notes in Computer Science (including subseries Lecture Notes in Artificial Intelligence and Lecture Notes in Bioinformatics), vol. 7577 LNCS, no. PART 6, 2012, pp. 100–114.
- [28] K. Yamaguchi, A. C. Berg, L. E. Ortiz, and T. L. Berg, "Who are you with and where are you going?" in Cvpr 2011, 2011, pp. 1345–1352.
- [29] K. Shafique, W. L. Mun, and N. Haering, "A rank constrained continuous formulation of multi-frame multi-target tracking problem," in 26th IEEE Conference on Computer Vision and Pattern Recognition, CVPR, 2008.
- [30] Q. Yu, G. Medioni, and I. Cohen, "Multiple Target Tracking Using Spatio-Temporal Markov Chain Monte Carlo Data Association,"

- in 2007 IEEE Conference on Computer Vision and Pattern Recognition, 2007, pp. 1–8.
- [31] R. Nevatia, "Multi-target tracking by online learning of nonlinear motion patterns and robust appearance models," in *Proceedings of the 2012 IEEE Conference on Computer Vision and Pattern Recognition (CVPR).* IEEE, 2012, pp. 1918–1925.
- [32] G. Ning, Z. Zhang, C. Huang, Z. He, X. Ren, and H. Wang, "Spatially Supervised Recurrent Convolutional Neural Networks for Visual Object Tracking," 2016.
- [33] Y. LeCun, Y. Bengio, and G. Hinton, "Deep learning," *Nature*, vol. 521, no. 7553, pp. 436–444, 2015.
- [34] J. Munkres, "Algorithms for the Assignment and Transportation Problems," Journal of the Society for Industrial and Applied Mathematics, vol. 5, no. 1, pp. 32–38, 1957.
- [35] L. Leal-Taixé, A. Milan, I. Reid, S. Roth, and K. Schindler, "MOTChallenge 2015: Towards a Benchmark for Multi-Target Tracking," pp. 1–15, 2015.
- [36] A. Milan, L. Leal-Taixé, I. D. Reid, S. Roth, and K. Schindler, "MOT16: A Benchmark for Multi-Object Tracking," CoRR, vol. abs/1603.0, 2016.
- [37] L. Wen, D. Du, Z. Cai, Z. Lei, M.-C. Chang, H. Qi, J. Lim, M.-H. Yang, and S. Lyu, "UA-DETRAC: A New Benchmark and Protocol for Multi-Object Detection and Tracking," 2015.
- [38] S. Lyu, M. C. Chang, D. Du, L. Wen, H. Qi, Y. Li, Y. Wei, L. Ke, T. Hu, M. Del Coco, P. Carcagni, D. Anisimov, E. Bochinski, F. Galasso, F. Bunyak, G. Han, H. Ye, H. Wang, K. Palaniappan, K. Ozcan, L. Wang, L. Wang, M. Lauer, N. Watcharapinchai, N. Song, N. M. Al-Shakarji, S. Wang, S. Amin, S. Rujikietgumjorn, T. Khanova, T. Sikora, T. Kutschbach, V. Eiselein, W. Tian, X. Xue, X. Yu, Y. Lu, Y. Zheng, Y. Huang, and Y. Zhang, "UA-DETRAC 2017: Report of AVSS2017 & IWT4S Challenge on Advanced Traffic Monitoring," in 2017 14th IEEE International Conference on Advanced Video and Signal Based Surveillance, AVSS 2017, 2017.
- [39] W. Luo, J. Xing, A. Milan, X. Zhang, W. Liu, X. Zhao, and T.-K. Kim, "Multiple Object Tracking: A Literature Review," arXiv:1409.7618v4, pp. 1–18, 2017.
- [40] P. Emami, P. M. Pardalos, L. Elefteriadou, and S. Ranka, "Machine Learning Methods for Solving Assignment Problems in Multi-Target Tracking," vol. 1, no. 1, pp. 1–35, 2018.
- [41] Y. Tian, A. Dehghan, and M. Shah, "On detection, data association and segmentation for multi-target tracking," IEEE Transactions on Pattern Analysis and Machine Intelligence, pp. 1–1, 2018.
- [42] K. Shafique and M. Shah, "A noniterative greedy algorithm for multiframe point correspondence," *IEEE transactions on pattern* analysis and machine intelligence, vol. 27, no. 1, pp. 51–65, 2005.
- [43] D. Reid et al., "An algorithm for tracking multiple targets," IEEE transactions on Automatic Control, vol. 24, no. 6, pp. 843–854, 1979.
- [44] G. Shu, A. Dehghan, O. Oreifej, E. Hand, and M. Shah, "Part-based multiple-person tracking with partial occlusion handling," in Computer Vision and Pattern Recognition (CVPR), 2012 IEEE Conference on. IEEE, 2012, pp. 1815–1821.
- [45] A. Roshan Zamir, A. Dehghan, and M. Shah, "GMCP-tracker: Global multi-object tracking using generalized minimum clique graphs," in Lecture Notes in Computer Science (including subseries Lecture Notes in Artificial Intelligence and Lecture Notes in Bioinformatics), 2012.
- [46] B. Wu and R. Nevatia, "Detection and tracking of multiple, partially occluded humans by bayesian combination of edgelet based part detectors," *International Journal of Computer Vision*, vol. 75, no. 2, pp. 247–266, 2007.
- [47] A. Dehghan, S. Modiri Assari, and M. Shah, "Gmmcp tracker: Globally optimal generalized maximum multi clique problem for multiple object tracking," in *Proceedings of the IEEE Conference on Computer Vision and Pattern Recognition*, 2015, pp. 4091–4099.
- [48] H. Pirsiavash, D. Ramanan, and C. C. Fowlkes, "Globally-optimal greedy algorithms for tracking a variable number of objects," Proceedings of the IEEE Computer Society Conference on Computer Vision and Pattern Recognition, pp. 1201–1208, 2011.
- [49] A. A. Butt and R. T. Collins, "Multi-target tracking by lagrangian relaxation to min-cost network flow," in *Proceedings of the IEEE Conference on Computer Vision and Pattern Recognition*, 2013, pp. 1846–1853.
- [50] J. Berclaz, F. Fleuret, E. Türetken, and P. Fua, "Multiple object tracking using k-shortest paths optimization," *IEEE Transactions* on Pattern Analysis and Machine Intelligence, vol. 33, no. 9, pp. 1806–1819, 2011.

- [51] H. B. Shitrit, J. Berclaz, F. Fleuret, and P. Fua, "Multi-commodity network flow for tracking multiple people," *IEEE transactions on* pattern analysis and machine intelligence, vol. 36, no. 8, pp. 1614– 1627, 2014.
- [52] V. Chari, S. Lacoste-Julien, I. Laptev, and J. Sivic, "On pairwise costs for network flow multi-object tracking," Proceedings of the IEEE Computer Society Conference on Computer Vision and Pattern Recognition, vol. 07-12-June, pp. 5537–5545, 2015.
- [53] P. F. Felzenszwalb, R. B. Girshick, D. McAllester, and D. Ramanan, "Object detection with discriminatively trained part-based models," *IEEE transactions on pattern analysis and machine intelligence*, vol. 32, no. 9, pp. 1627–1645, 2010.
- [54] B. Leibe, K. Schindler, N. Cornelis, and L. Van Gool, "Coupled object detection and tracking from static cameras and moving vehicles," *IEEE transactions on pattern analysis and machine intelligence*, vol. 30, no. 10, pp. 1683–1698, 2008.
- [55] S. Tang, B. Andres, M. Andriluka, and B. Schiele, "Subgraph decomposition for multi-target tracking," in *Proceedings of the IEEE Conference on Computer Vision and Pattern Recognition*, 2015, pp. 5033–5041.
- pp. 5033–5041.
  [56] Z. Kalal, K. Mikolajczyk, and J. Matas, "Tracking-Learning-Detection." *IEEE transactions on pattern analysis and machine intelligence*, vol. 34, no. 7, pp. 1409–1422, 2011.
- [57] S. Hare, A. Saffari, and P. H. Torr, "Struck: Structured output tracking with kernels," in *Computer Vision (ICCV)*, 2011 IEEE International Conference on. IEEE, 2011, pp. 263–270.
- [58] S. Wang, H. Lu, F. Yang, and M.-H. Yang, "Superpixel tracking," 2011.
- [59] L. Zhang and L. van der Maaten, "Structure preserving object tracking," in Proceedings of the IEEE conference on computer vision and pattern recognition, 2013, pp. 1838–1845.
- [60] A. Milan, S. Roth, and K. Schindler, "Continuous energy minimization for multitarget tracking," IEEE Transactions on Pattern Analysis and Machine Intelligence, vol. 36, no. 1, pp. 58–72, 2014.
- [61] E. Bochinski, V. Eiselein, and T. Sikora, "High-Speed tracking-by-detection without using image information," in 2017 14th IEEE International Conference on Advanced Video and Signal Based Surveillance, AVSS 2017, 2017.
- [62] J. Chen, H. Sheng, Y. Zhang, and Z. Xiong, "Enhancing Detection Model for Multiple Hypothesis Tracking," in 2017 IEEE Conference on Computer Vision and Pattern Recognition Workshops (CVPRW), 2017, pp. 2143–2152.
- [63] L. Bertinetto, J. Valmadre, J. F. Henriques, A. Vedaldi, and P. H. Torr, "Fully-convolutional siamese networks for object tracking," Lecture Notes in Computer Science, vol. 9914 LNCS, pp. 850–865, 2016.
- [64] J. Son, M. Baek, M. Cho, and B. Han, "Multi-Object Tracking with Quadruplet Convolutional Neural Networks," Cvpr, pp. 5620– 5629, 2017.
- [65] S. Schulter, P. Vernaza, W. Choi, and M. Chandraker, "Deep Network Flow for Multi-Object Tracking," Cvpr, pp. 6951–6960, 2017.
- [66] C. Feichtenhofer, A. Pinz, and A. Zisserman, "Detect to Track and Track to Detect," Proceedings of the IEEE International Conference on Computer Vision, vol. 2017-Octob, pp. 3057–3065, 2017.
- [67] E. Insafutdinov, M. Andriluka, L. Pishchulin, S. Tang, E. Levinkov, B. Andres, and B. Schiele, "ArtTrack: Articulated multi-person tracking in the wild," Proceedings - 30th IEEE Conference on Computer Vision and Pattern Recognition, CVPR 2017, vol. 2017-Janua, pp. 1293–1301, 2017.
- [68] S. Chopra, R. Hadsell, and Y. LeCun, "Learning a similarity metric discriminatively, with application to face verification," Proceedings of the IEEE Computer Society Conference on Computer Vision and Pattern Recognition, vol. 1, pp. 539–546, 2005.
- [69] S. Hershey, S. Chaudhuri, D. P. Ellis, J. F. Gemmeke, A. Jansen, R. C. Moore, M. Plakal, D. Platt, R. A. Saurous, B. Seybold, M. Slaney, R. J. Weiss, and K. Wilson, "CNN architectures for large-scale audio classification," ICASSP, IEEE International Conference on Acoustics, Speech and Signal Processing Proceedings, no. Nips, pp. 131–135, 2017.
- [70] A. Milan, L. Leal-Taixe, I. Reid, S. Roth, and K. Schindler, "MOT16: A Benchmark for Multi-Object Tracking," pp. 1–12, 2016.
- [71] A. Geiger, P. Lenz, and R. Urtasun, "Are we ready for autonomous driving? the KITTI vision benchmark suite," in Proceedings of the IEEE Computer Society Conference on Computer Vision and Pattern Recognition, 2012, pp. 3354–3361.

- [72] L. Patino, T. Cane, A. Vallee, and J. Ferryman, "PETS 2016: Dataset and Challenge," in *IEEE Computer Society Conference on Computer Vision and Pattern Recognition Workshops*, 2016, pp. 1240–1247.
- [73] L. Wang, Y. Lu, H. Wang, Y. Zheng, H. Ye, and X. Xue, "Evolving boxes for fast vehicle detection," *Proceedings - IEEE International Conference on Multimedia and Expo*, pp. 1135–1140, 2017.
- [74] F. Yang, W. Choi, and Y. Lin, "Exploit All the Layers: Fast and Accurate CNN Object Detector with Scale Dependent Pooling and Cascaded Rejection Classifiers," in 2016 IEEE Conference on Computer Vision and Pattern Recognition (CVPR), 2016, pp. 2129– 2137.
- [75] P. Dollar, R. Appel, S. Belongie, and P. Perona, "Fast feature pyramids for object detection," IEEE Transactions on Pattern Analysis and Machine Intelligence, 2014.
- [76] W. Liu, D. Anguelov, D. Erhan, C. Szegedy, S. Reed, C. Y. Fu, and A. C. Berg, "SSD: Single shot multibox detector," *Lecture Notes in Computer Science (including subseries Lecture Notes in Artificial Intelligence and Lecture Notes in Bioinformatics)*, vol. 9905 LNCS, pp. 21–37, 2016.
- [77] K. Simonyan and A. Zisserman, "Very Deep Convolutional Networks for Large-Scale Image Recognition," International Conference on Learning Representations (ICRL), pp. 1–14, 2015.
- [78] S. Ioffe and C. Szegedy, "Batch normalization: Accelerating deep network training by reducing internal covariate shift," arXiv preprint arXiv:1502.03167, 2015.
- [79] V. Nair and G. E. Hinton, "Rectified Linear Units Improve Restricted Boltzmann Machines," Proceedings of the 27th International Conference on Machine Learning, no. 3, pp. 807–814, 2010.
- [80] K. Bernardin and R. Stiefelhagen, "Evaluating multiple object tracking performance: The CLEAR MOT metrics," Eurasip Journal on Image and Video Processing, vol. 2008, 2008.
- [81] E. Ristani, F. Solera, R. Zou, R. Cucchiara, and C. Tomasi, "Performance measures and a data set for multi-target, multicamera tracking," in Lecture Notes in Computer Science (including subseries Lecture Notes in Artificial Intelligence and Lecture Notes in Bioinformatics), vol. 9914 LNCS, 2016, pp. 17–35.
- [82] Y. Li, C. Huang, and R. Nevatia, "Learning to associate: Hybridboosted multi-target tracker for crowded scene," in 2009 IEEE Computer Society Conference on Computer Vision and Pattern Recognition Workshops, CVPR Workshops 2009, 2009, pp. 2953–2960.
- [83] M. Keuper, S. Tang, Y. Zhongjie, B. Andres, T. Brox, and B. Schiele, "A Multi-cut Formulation for Joint Segmentation and Tracking of Multiple Objects," CoRR, vol. abs/1607.0, 2016.
- [84] C. Kim, F. Li, and J. Rehg, "Multi-object Tracking with Neural Gating Using Bilinear LSTM," in *Proceedings of the European Conference on Computer Vision (ECCV)*, 2018, pp. 200–215.
- [85] R. Sanchez-Matilla, F. Poiesi, and A. Cavallaro, "Online Multitarget Tracking with Strong and Weak Detections," in *Computer Vision – ECCV 2016 Workshops*, G. Hua and H. Jégou, Eds. Cham: Springer International Publishing, 2016, pp. 84–99.
- [86] V. Eiselein, D. Arp, M. Pätzold, and T. Sikora, "Real-time multihuman tracking using a probability hypothesis density filter and multiple detectors," in *Proceedings - 2012 IEEE 9th International* Conference on Advanced Video and Signal-Based Surveillance, AVSS 2012, 2012, pp. 325–330.
- [87] B. Wang, L. Wang, B. Shuai, Z. Zuo, T. Liu, K. L. Chan, and G. Wang, "Joint Learning of Convolutional Neural Networks and Temporally Constrained Metrics for Tracklet Association," in IEEE Computer Society Conference on Computer Vision and Pattern Recognition Workshops, 2016.
- [88] L. Leal-Taixe, C. Canton-Ferrer, and K. Schindler, "Learning by Tracking: Siamese CNN for Robust Target Association," in IEEE Computer Society Conference on Computer Vision and Pattern Recognition Workshops, 2016.
- [89] S. Wang and C. C. Fowlkes, "Learning Optimal Parameters for Multi-target Tracking with Contextual Interactions," *International Journal of Computer Vision*, 2017.
- [90] A. Sadeghian, A. Alahi, and S. Savarese, "Tracking the Untrackable: Learning to Track Multiple Cues with Long-Term Dependencies," in *Proceedings of the IEEE International Conference on Computer Vision*, 2017.
- [91] Q. Chu, W. Ouyang, H. Li, X. Wang, B. Liu, and N. Yu, "Online Multi-object Tracking Using CNN-Based Single Object Tracker with Spatial-Temporal Attention Mechanism," in *Proceedings of the IEEE International Conference on Computer Vision*, 2017.

- [92] J. H. Yoon, C.-R. Lee, M.-H. Yang, and K.-J. Yoon, "Online Multiobject Tracking via Structural Constraint Event Aggregation," in 2016 IEEE Conference on Computer Vision and Pattern Recognition (CVPR), 2016.
- [93] A. Milan, S. H. Rezatofighi, A. Dick, K. Schindler, and I. Reid, "Online Multi-target Tracking using Recurrent Neural Networks," Arxiv, 2016.
- [94] R. Girshick, J. Donahue, T. Darrell, and J. Malik, "Rich feature hierarchies for accurate object detection and semantic segmentation," in *Proceedings of the IEEE Computer Society Conference on Computer Vision and Pattern Recognition*, 2014.
- [95] Z. Cai, M. Saberian, and N. Vasconcelos, "Learning complexity-aware cascades for deep pedestrian detection," in *Proceedings of the IEEE International Conference on Computer Vision*, vol. 2015 Inter, 2015, pp. 3361–3369.
- [96] A. Andriyenko, K. Schindler, and S. Roth, "Discrete-continuous optimization for multi-target tracking," in *Proceedings of the IEEE Computer Society Conference on Computer Vision and Pattern Recognition*, 2012, pp. 1926–1933.
- nition, 2012, pp. 1926–1933.

  [97] C. Dicle, O. I. Camps, and M. Sznaier, "The way they move: Tracking multiple targets with similar appearance," in *Proceedings of the IEEE International Conference on Computer Vision*, 2013, pp. 2304–2311.
- [98] A. Andriyenko and K. Schindler, "Multi-target tracking by continuous energy minimization," in Proceedings of the IEEE Computer Society Conference on Computer Vision and Pattern Recognition, 2011, pp. 1265–1272.
- [99] A. Paszke, G. Chanan, Z. Lin, S. Gross, E. Yang, L. Antiga, and Z. Devito, "Automatic differentiation in PyTorch," Advances in Neural Information Processing Systems 30, no. Nips, pp. 1–4, 2017.
- [100] S. Zhang, A. E. Choromanska, and Y. LeCun, "Deep learning with elastic averaging SGD," in Advances in Neural Information Processing Systems, 2015, pp. 685–693.



HuanSheng Song received the B.S. and M.S. degrees in communication and electronic systems and the Ph.D. degree in information and communication engineering from Xian Jiaotong University, Xian, China, in 1985, 1988, and 1996, respectively. Since 2004, he has been with the Information Engineering Institute, Changan University, Xian, where he became a Professor in 2006 and was nominated as the Dean in 2012. He has been involved in research on intelligent transportation systems for many years and has

led a research team to develop a vehicle license plate reader and a traffic event detection system based on videos, which has brought about complete industrialization. His current research interests include image processing and recognition, as well as intelligent transportation systems.



Ajmal Mian completed his PhD from The University of Western Australia in 2006 with distinction and received the Australasian Distinguished Doctoral Dissertation Award from Computing Research and Education Association of Australasia. He received the prestigious Australian Postdoctoral and Australian Research Fellowships in 2008 and 2011 respectively. He received UWA Outstanding Young Investigator Award 2011, West Australian Early Career Scientist of the Year 2012 award, Vice-Chancellor's

Mid-Career Research Award 2014, EH Tompson Award 2015, Aspire Professional Development Award 2016 and Excellence in Research Supervision award 2017. He has secured eight Australian Research Council grants, a National Health and Medical Research Council grant and a DAAD German Australian Cooperation grant. He is currently a Professor of Computer Science at The University of Western Australia. His research interests include computer vision, machine learning, face recognition, 3D shape analysis and video understanding.



ShiJie Sun received his B.S. in software engineering from The University of Chang'an University and is currently working towards the Ph.D. degree in intelligent transportation and information system engineering with Chang'an University. Currently, he is a visiting (joint) Ph.D. candidate at the University of Western Australia since October 2017. His research interests include machine learning, object detection, localization & tracking, action recognition.



Naveed Akhtar received his PhD in Computer Vision from The University of Western Australia (UWA) and Master degree in Computer Science from Hochschule Bonn-Rhein-Sieg, Germany. His research in Computer Vision is regularly published in IEEE CVPR, ECCV and IEEE TPAMI. He has also served as a reviewer for over ten reputed journals in this field. Currently, he is a Research Fellow at UWA. He also served on the same position at the Australian National University in the past. His research interests include

object tracking, action recognition, and hyperspectral image analysis.



Mubarak Shah the trustee chair professor of computer science, is the founding director of the Center for Research in Computer Vision at University of Central Florida. He is an editor of an international book series on video computing, was editor-in-chief of Machine Vision and Applications journal, and an associate editor of ACM Computing Surveys journal. His research interests include video surveillance, visual tracking, human activity recognition, visual analysis of crowded scenes, video registration, UAV video

analysis, and so on. He is a fellow of the IEEE, AAAS, IAPR, and SPIE